Carboxyamidotriazole-induced inhibition of mitochondrial calcium import blocks capacitative calcium entry and cell proliferation in HEK-293 cells

Olivier Mignen[1], Christine Brink[2], Antoine Enfissi[3,4], Aditi Nadkarni[2], Trevor J. Shuttleworth[1], David R. Giovannucci[2] and Thierry Capiod[3,4,*]

[1]Department of Pharmacology and Physiology, University of Rochester, 601 Elmwood Avenue, Rochester, NY 14642, USA
[2]Department of Neuroscience, Medical College of Ohio, 3036 Arlington Avenue, Toledo, OH 43614, USA
[3]INSERM, EMI 0228, IFR118, Université des Sciences et Technologies de Lille 1, Bât. SN3, 59655 Villeneuve d'Ascq CEDEX, France
[4]INSERM, U442, IFR46, Université Paris-Sud, Bât.443, 91405 Orsay CEDEX, France
*Author for correspondence (e-mail: thierry.capiod@univ-lille1.fr)

Accepted 25 August 2005
Journal of Cell Science 118, 5615-5623 Published by The Company of Biologists 2005
doi:10.1242/jcs.02663

Summary

Blocking calcium entry may prevent normal and pathological cell proliferation. There is evidence suggesting that molecules such as carboxyamidotriazole, widely used in anti-cancer therapy based on its ability to block calcium entry in nonexcitable cells, also have antiproliferative properties. We found that carboxyamidotriazole and the capacitative calcium entry blocker 2-aminoethoxydiphenyl borate inhibited proliferation in HEK-293 cells with IC_{50} values of 1.6 and 50 μM, respectively. Capacitative calcium entry is activated as a result of intracellular calcium store depletion. However, non-capacitative calcium entry pathways exist that are independent of store depletion and are activated by arachidonic acid and diacylglycerol, generated subsequent to G protein coupled receptor stimulation. We found that carboxyamidotriazole completely inhibited the capacitative calcium entry and had no effect on the amplitude of arachidonic-acid-activated non-capacitative calcium entry. However, investigation of the effects of carboxyamidotriazole on mitochondrial calcium dynamics induced by carbachol, capacitative calcium entry and exogenously set calcium loads in intact and digitonin-permeabilized cells revealed that carboxyamidotriazole inhibited both calcium entry and mitochondrial calcium uptake in a time-dependent manner. Mitochondrial inner-membrane potential was altered by carboxyamidotriazole treatment, suggesting that carboxyamidotriazole antagonizes mitochondrial calcium import and thus local calcium clearance, which is crucial for the maintenance of capacitative calcium entry.

Key words: CAI, 2-APB, CCE, Mitochondrial respiration, ARC

Introduction

Two main calcium entry pathways have been identified in nonexcitable cells: non-capacitative calcium entry (NCCE) and capacitative (or store-operated) calcium entry (CCE) (Bird et al., 2004; Parekh and Putney, 2005). Depletion of intracellular calcium stores is needed to activate CCE, whereas NCCE is activated by intracellular second messengers, such as DAG and arachidonic acid (AA), and is independent of store depletion. Recent evidence has indicated that NCCE is specifically activated at low agonist concentrations, whereas CCE only occurs at high agonist concentrations: a phenomenon described as the reciprocal regulation of Ca^{2+} entry (Mignen et al., 2001). CCE is thought to be an essential component of the long-term responses of the cell, including proliferation (Enfissi et al., 2004; Golovina, 1999; Golovina et al., 2001; Sweeney et al., 2002; Yu et al., 2003). Normal and pathological cell proliferation may be prevented by blocking calcium influx and there is some evidence suggesting that molecules that block calcium entry also have antiproliferative properties (Haverstick et al., 2000; Kohn and Liotta, 1990). Carboxyamidotriazole (CAI) has such properties in model systems in vitro and in vivo (Alessandro et al., 1996). CAI is a potential anti-cancer drug, and phase II clinical trials are already underway in human patients (Hussain et al., 2003; Kohn et al., 1997). In the human hepatoma cells Hep G2 and Huh-7, CAI and 2-aminoethoxydiphenyl borate (2-APB), another non-specific CCE blocker, inhibit both CCE and cell proliferation (Enfissi et al., 2004). However, CAI and 2-APB have numerous effects on the regulation of cellular calcium and these effects are not specific to CCE (Felder et al., 1991; Peppiatt et al., 2003). There is only a limited amount of evidence indicating that NCCE is involved in the regulation of cell proliferation (Thebault et al., 2003), but it is not known whether CAI can also block NCCE. Earlier studies using CAI as a calcium entry blocker showed that pre-treatment is required for complete inhibition, suggesting that CAI does not directly block calcium channels. CCE has been shown to modulate mitochondrial Ca^{2+} uptake (Gilabert and Parekh, 2000; Hoth et al., 1997). Respiring mitochondria buffer Ca^{2+} and reduce Ca^{2+} inactivation of CCE, whereas depolarization of mitochondria using CCCP or oligomycin lowers Ca^{2+} uptake and inhibits CCE. Therefore, we investigated here whether CAI interferes with these organelles to control CCE in HEK-293 cells. Our results suggest that CAI antagonizes mitochondrial calcium import and thus local

calcium clearance, which is crucial for the maintenance of CRAC (calcium-release-activated calcium) channel function and CCE. In addition, we show that CAI does not affect the NCCE pathway involving the arachidonate-regulated Ca^{2+}-selective ARC channels (Mignen and Shuttleworth, 2000; Mignen et al., 2005a; Mignen et al., 2005b), thereby providing evidence that the regulation of these specific calcium channels does not imply a role for mitochondria.

The blocking effect of CAI on CCE would explain its role in cell proliferation, which mainly depends on the activation of this specific calcium-entry pathway. However, the actual mechanism by which it occurs may limit the therapeutic usefulness of this molecule.

Materials and Methods

Cell proliferation

HEK-293 cells were plated in 24-well plates at a density of 30,000 cells/cm^2 in complete medium (Earle's MEM with Glutamax-I) supplemented with 10% fetal calf serum (FCS), penicillin (200,000 U/ml) and streptomycin (100 μg/ml) (Life Technologies, Cergy-Pontoise, France). The cells were incubated for 24 hours at 37°C in a humidified atmosphere containing 5% CO_2, and then for a further 24 hours with or without FCS, in the presence or absence of various concentrations of CAI or 2-APB. The cells were labeled with 0.2 μCi/ml [methyl-^{3}H]thymidine for the last 4 hours, and proteins were precipitated using TCA (trichloroacetic acid). The precipitate was then subjected to counting in a scintillation counter.

Calcium measurements

HEK-293 cells (5×10^6 cells/ml) were loaded with 4 μM Fura-2/AM in complete culture medium for 45 minutes at 37°C. Cells were treated with trypsin and washed once by centrifugation at 300 ***g*** for 1 minute in the same medium. Cell pellets were resuspended in 116 mM NaCl, 5.6 mM KCl, 1.2 mM $MgCl_2$, 1 mM NaH_2PO_4, 5 mM $NaHCO_3$, 0.1 mM EGTA, 20 mM HEPES, pH 7.3. Cell suspensions were transferred to a quartz cuvette and placed in the light beam of a Hitachi F2000 spectrofluorimeter, with continuous stirring, at 37°C. Changes in $[Ca^{2+}]_i$ were recorded by measuring increases in the ratio of the readings obtained at excitation wavelengths of 340 and 380 nm.

Optical assessment of mitochondrial membrane potential (ψ_m)

HEK-293 cells were incubated in phosphate-buffered saline (PBS) (Gibco, Rockville, MD) supplemented with 2 μg/ml JC-1 (5,5′,6,6′-tetrachloro-1,1′,3,3′-tetraethylbenzimidazolylcarbocyanine iodide) for 30 minutes at room temperature in the dark. Cells were then centrifuged at 1200 ***g*** for 5 minutes and resuspended in dye-free physiological saline solution (PSS) containing 140 mM NaCl, 5 mM KCl, 1 mM $MgCl_2$, 2.2 mM $CaCl_2$, 10 mM HEPES, 10 mM Glucose, pH 7.2. The cells (100,000 cells/well) were then placed in 48-well culture plates (Corning plate 3548). A Fluostar Optima multi-well plate reader (BMG Labtechnologies, Durham, NC) was used to detect the fluorescence emission at 590 nm and 520 nm in response to alternating 530 nm and 485 nm excitation, respectively.

Mn^{2+} quenching

The entry of Ca^{2+} into individual intact cells was measured as the rate at which intracellular indo-1 was quenched by Mn^{2+}, as previously described (Shuttleworth and Thompson, 1999).

Electrophysiological recordings

Macroscopic whole-cell currents were recorded using an Axopatch 1-C patch-clamp amplifier (Axon Instruments, Foster City, CA, USA) as previously described (Mignen and Shuttleworth, 2000).

Monitoring mitochondrial calcium dynamics

HEK-293 cells stably expressing the m3 muscarinic receptor (kind gift of Craig Logsdon, University of Michigan Medical School, Ann Arbor, MI) were grown in DMEM supplemented with 10% FCS, penicillin (200,000 U/ml) and streptomycin (100 μg/ml) (Gibco, Rockville, MD) on 25×25 mm clean glass coverslips, which formed the bottom of a perfusion chamber. Cells were loaded with 2 μM Rhod-2/AM, Rhod-FF/AM and Rhod-5N/AM mixture in PSS for 30 minutes at room temperature in the dark. Cells were then permeabilized for 3 minutes at 37°C in an intracellular saline solution (ISS) containing 10 μM digitonin but no added Ca^{2+}. The ISS contained 130 mM KCl, 10 mM NaCl, 1 mM K_3PO_4, 1 mM ATP, 0.02 mM ADP, 2 mM succinate, 20 mM HEPES, 2 mM $MgCl_2$ (adjusted to buffer Ca^{2+}). Intracellular saline solutions with specific set calcium concentrations were obtained by adding HEDTA/Ca^{2+}. EGTA (250 μM) was added to the 'zero'-Ca^{2+} solution, pH 6.8. The Ca^{2+} challenge solutions (containing 3-3000 μM Ca^{2+}) were exchanged using a pressure-driven perfusion system. Changes in $[Ca^{2+}]_m$ were monitored by digital fluorescence imaging on a Nikon TE2000-S inverted fluorescence microscope (Nikon, Melville, NY) equipped with a monochrometer-based imaging system (TILL Photonics, Martinsried, Germany) and a Nikon 40× SuperFluor oil-immersion objective lens, NA 1.3. All fluorescent data were converted to $\Delta F/F_0=100[(F-F_0)/F_0]$, where F is the recorded fluorescence and F_0 is the average of the first 15 frames of data. Full-frame images were collected at 1 second intervals for at least 400 seconds and changes are expressed as the percentage increase compared with F_0.

TMRE plate reader analysis

HEK-293 cells were loaded with 1.5 μM TMRE (tetramethylrhodamine ethyl ester perchlorate) in PSS for 15 minutes at room temperature in the dark. Dye was then washed with fresh dye-free PSS and spun down at 300 ***g*** for 5 minutes. Cells were then resuspended in 24 ml PSS, loaded onto a 24-well plate at 1 ml per well, and allowed to rest for 30 minutes prior to monitoring by fluorescent plate reader. Cells were excited with 544 nm light and emission was measured at 590 nm. Wells were measured at 1 minute intervals for 10 minutes prior to treatment. Wells were then treated with 0 μM CAI (control), 10 μM CAI or 20 μM carbonyl cyanide 4-trifluoromethoxyphenyl-hydrazone (FCCP) and monitoring was resumed for an additional 30 minutes.

TMRE digital imaging analysis

HEK-293 cells were loaded on coverslips with 12.5 nM TMRE in PSS for 15 minutes at 37°C in the dark. Cells were then washed with PSS and kept at room temperature for 30 minutes before measuring to allow the dye to concentrate in the mitochondria. Following loading, coverslips were mounted in chambers and monitored by digital fluorescence imaging at 1 Hz. Solution changes were achieved by bath perifusion.

In some experiments $[Ca^{2+}]_m$ was measured using a multi-well plate reader. In these experiments, HEK-293 cells were loaded with 200 nM MitoTracker Green FM and 1 μM Rhodamine mixture for 10 minutes, and permeabilized with digitonin. Cells were resuspended in ISS, and half of the cells were incubated with 10 μM CAI for 30 minutes. A Fluostar Optima multi-well fluorescence plate reader (BMG Labtechnologies) was used as described above. Following the addition of Ca^{2+} to each well, the 590/520 nm ratio was monitored at 5 minute intervals.

Confocal microscopy

Images of JC-1-labeled mitochondria were obtained using a Zeiss 510 Meta laser-scanning confocal microscope equipped with an Axiovert 200 MOT microscope with a 63×/NA 1.4 Plan-Apo oil-immersion objective. JC-1 dye was alternately excited with the 488 nm and 543 nm laser lines.

Chemicals

CAI was a gift from the Drug Synthesis and Chemistry Branch, National Cancer Institute (Bethesda, MD) and 2-APB was a gift from Yves Chapleur (CNRS UMR 7565, Nancy, France). Thapsigargin was obtained from Alomone Labs (Jerusalem, Israel), [methyl-^{3}H]thymidine (25 Ci/mmol) was obtained from Amersham Pharmacia Biotech and Fura-2/AM from Molecular Probes Europe). All other reagents were from Sigma (St Louis, MI). All ion-sensitive dyes and mitochondrial probes were purchased from Molecular Probes (Leiden, The Netherlands).

Results

Effects of CAI and 2-APB on the amplitude of CCE

We assessed the ability of CAI and 2-APB to block CCE in suspensions of HEK-293 cells loaded with Fura-2/AM. Cell pellets were resuspended in a Ca^{2+}-free medium containing 100 μM EGTA, in the presence or absence of 1 μM thapsigargin, which blocks the SERCA calcium pump. The addition of thapsigargin resulted in the depletion of intracellular Ca^{2+} stores within 4 to 6 minutes. The control cells were maintained in the absence of external calcium for the same time. We then added 2 mM Ca^{2+} to the cuvette and estimated the CCE amplitude as the difference between the $[Ca^{2+}]_i$ increase measured in the presence and in the absence of thapsigargin. CAI or 2-APB were added before calcium to investigate the abilities of these molecules to inhibit CCE and the amplitude of the CCE block was estimated as the peak of the $[Ca^{2+}]_i$ increase (Fig. 1). Half-maximal CCE inhibition was obtained with approximately 20 μM 2-APB and maximal effects were observed at 50 μM. The same pattern was observed when CCE was estimated from the rate of $[Ca^{2+}]_i$ increase (data not shown).

After 5 minutes in the presence of CAI, half-maximal CCE inhibition was observed at 0.5 μM and maximal CCE inhibition at approximately 2 μM. However, the amplitude of the inhibitory effect of CAI on CCE depended on the duration of application of the drug. When added 10 seconds before Ca^{2+}, 10 μM CAI reduced the CCE amplitude by 40%, whereas 10 μM CAI led to complete inhibition when added 5 minutes before Ca^{2+} (Fig. 2). The time-dependent CAI-evoked inhibitory effects on the CCE amplitude suggest that the calcium channels were inhibited by a complex mechanism. CAI had no effect on the $[Ca^{2+}]_i$ increase observed in the absence of thapsigargin (data not shown), indicating that CAI affected CCE only. Owing to the potentially toxic effects of CAI (Enfissi et al., 2004), we did not use concentrations exceeding 10 μM.

The time-dependence of CAI inhibition was confirmed in whole-cell voltage-clamped HEK-293 cells. Store-operated calcium currents (I_{SOC}) were examined in m3-expressing HEK-293 cells. Intracellular Ca^{2+} stores were depleted using a Ca^{2+}-free pipette solution and 2 μM adenophostin A. CAI (5 μM) was applied either 5 minutes before going whole-cell or at the peak of the inward current as shown on individual traces (Fig. 3A). The results are summarized in Fig. 3B. The magnitude of the resulting current, I_{SOC}, measured at –80 mV was 0.63±0.04 pA/pF (n=5). In cells pre-incubated with 5 μM CAI, the I_{SOC}

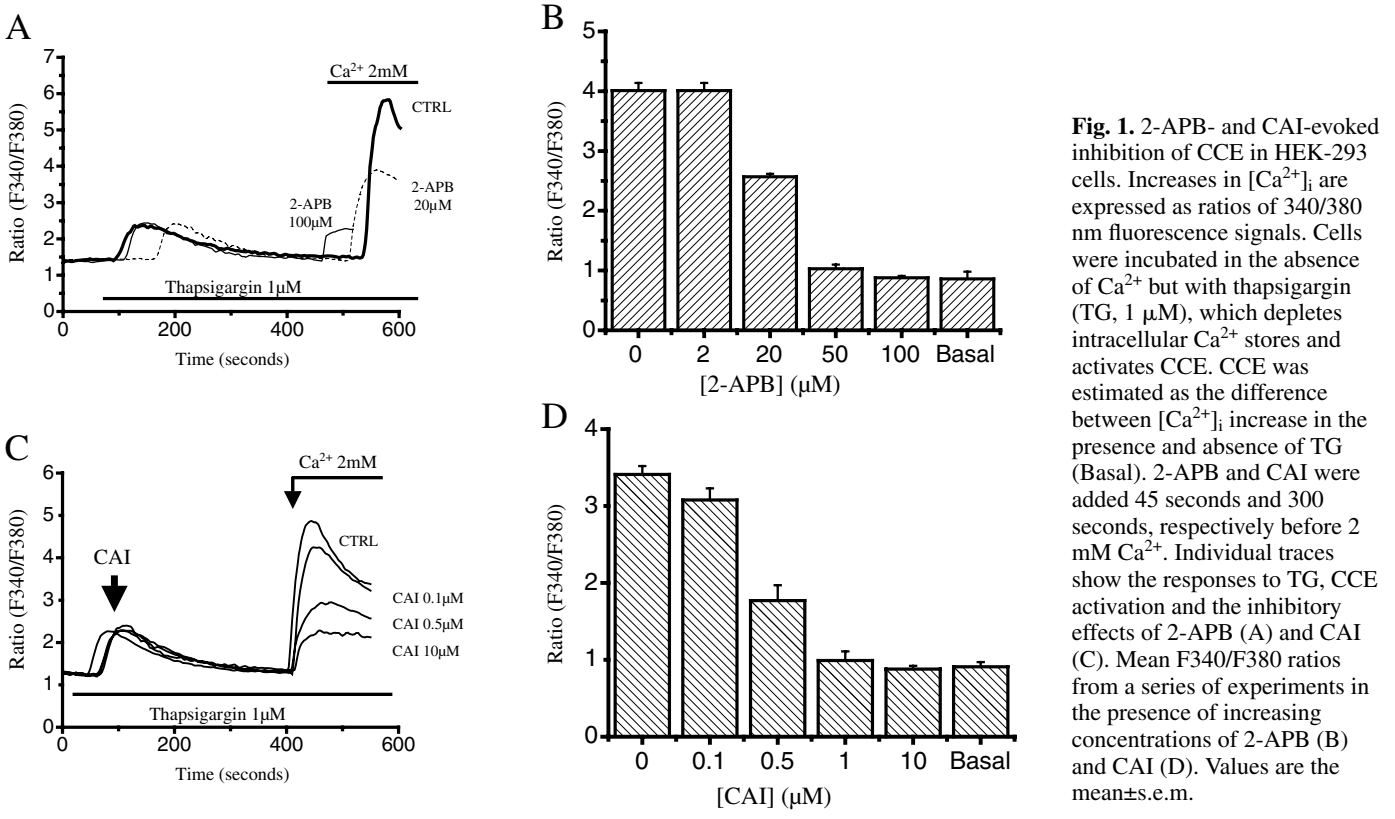

Fig. 1. 2-APB- and CAI-evoked inhibition of CCE in HEK-293 cells. Increases in $[Ca^{2+}]_i$ are expressed as ratios of 340/380 nm fluorescence signals. Cells were incubated in the absence of Ca^{2+} but with thapsigargin (TG, 1 μM), which depletes intracellular Ca^{2+} stores and activates CCE. CCE was estimated as the difference between $[Ca^{2+}]_i$ increase in the presence and absence of TG (Basal). 2-APB and CAI were added 45 seconds and 300 seconds, respectively before 2 mM Ca^{2+}. Individual traces show the responses to TG, CCE activation and the inhibitory effects of 2-APB (A) and CAI (C). Mean F340/F380 ratios from a series of experiments in the presence of increasing concentrations of 2-APB (B) and CAI (D). Values are the mean±s.e.m.

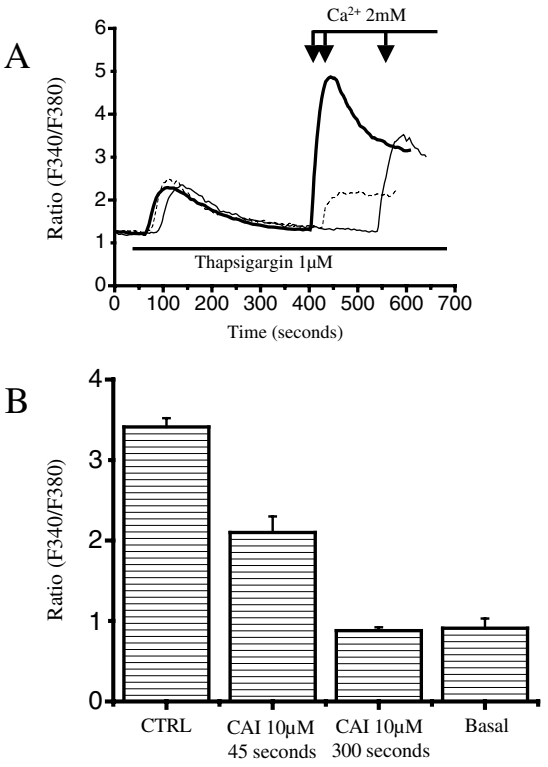

Fig. 2. Time-dependent effect of CAI on CCE inhibition. Thapsigargin (1 μM) and Ca^{2+} (2 mM) were added to a suspension of HEK-293 cells. (A) CAI (10 μM) was added either 45 seconds (thin solid trace) or 300 seconds (dashed line) before Ca^{2+} and the CCE increase was compared with that in control cells (thick solid trace) and the $[Ca^{2+}]_i$ increase in the absence of Ca^{2+} store depletion (basal, not shown). (B) Mean results from a series of experiments similar to those shown in A. Values are the mean±s.e.m.; *n*=39, 3, 10 and 4 for control, CAI 300 seconds, CAI 45 seconds and basal, respectively.

amplitude was 50% lower (0.30±0.02 pA/pF, *n*=5), whereas CAI had no effect when applied at the peak of the current (0.67±0.07 pA/pF, *n*=5).

Lack of effect of CAI on non-capacitative ARC channels

In addition to CCE, agonist-activated Ca^{2+} entry can occur via mechanisms independent of store depletion. One of these mechanisms is specifically activated by arachidonic acid and appears to be present in several different cell types (Mignen and Shuttleworth, 2000; Mignen et al., 2003; Mignen et al., 2005a; Mignen et al., 2005b). The channels responsible for this entry have been characterized and named ARC channels (for arachidonate-regulated Ca^{2+}-selective channels) (Mignen and Shuttleworth, 2000; Mignen et al., 2003). These channels appear to be specifically responsible for the entry of calcium (NCCE) following stimulation with a low concentration of agonist (Mignen et al., 2001). To compare the effect of CAI on CCE and on NCCE, we examined its effect on the rate of Mn^{2+} quench of intracellularly loaded indo-1 (as a surrogate for Ca^{2+} entry) in HEK-293 cells (Shuttleworth and Thompson, 1999). CAI was added approximately 7-10 minutes prior to the initiation of the quench measurements. The Mn^{2+} quench rate activated by exogenous arachidonic acid (8 μM) was unaffected by the addition of 5 μM CAI (quench rate 5.0±0.4% per minute, *n*=5 vs 3.8±0.6% per minute, *n*=4 in control cells). By contrast, in the same conditions, the rate of Mn^{2+} quench via CCE, as activated by addition of thapsigargin (1 μM), was reduced by more than 70% (1.1±0.4% per minute, *n*=4 vs 4.0±0.5% per minute, *n*=4 in control cells).

CAI depolarizes the mitochondrial inner-membrane potential in a time- and concentration-dependent manner

Mitochondria play a crucial role in the regulation of CCE by buffering local increases in cytosolic Ca^{2+} thereby limiting the Ca^{2+}-dependent inhibition of CCE channels (Gilabert and Parekh, 2000; Hoth et al., 1997). Consistent with this, we showed that activation of CCE induced an increase in intramitochondrial Ca^{2+} concentration, which was blocked by 20 μM FCCP, as measured in intact HEK-293 cells loaded with the mitochondrial-selective Rhod-2 dyes (Fig. 4A). As the ability of mitochondria to take up Ca^{2+} is dependent on the maintenance of a highly negative intramitochondrial membrane potential, we performed an initial set of experiments to determine the effect of CAI on this potential (ψ_m). The average change in ψ_m was measured in a multi-well

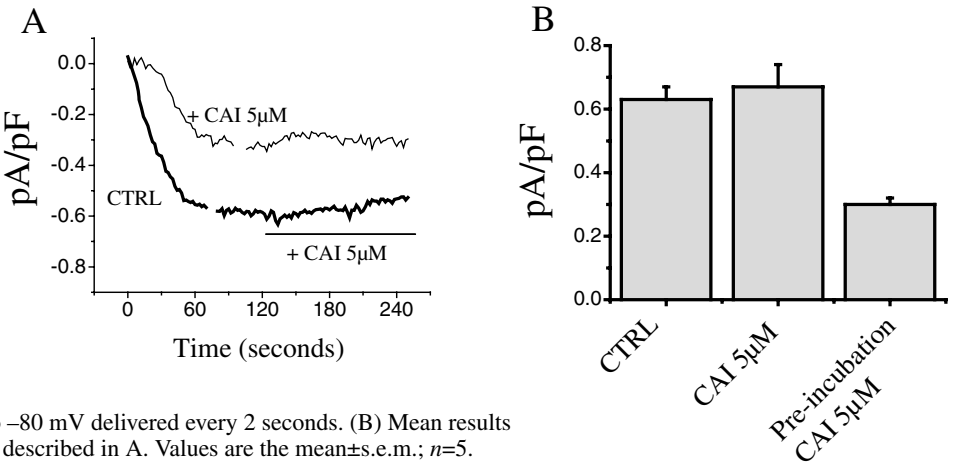

Fig. 3. CAI-induced inhibition of store-operated inward calcium currents. (A) HEK-293 cells were pre-incubated with 5 μM CAI (thin trace) or not (CTRL, thick trace). Gaps in the current traces correspond to the time taken to apply voltage ramps to determine current/potential relationships. The addition of 5 μM CAI (horizontal line) did not reduce the amplitude of the plateau phase of the inward current recorded in the control conditions. Whole-cell currents were measured using 250 millisecond voltage steps from a holding potential of 0 to –80 mV delivered every 2 seconds. (B) Mean results from a series of experiments similar to those described in A. Values are the mean±s.e.m.; *n*=5.

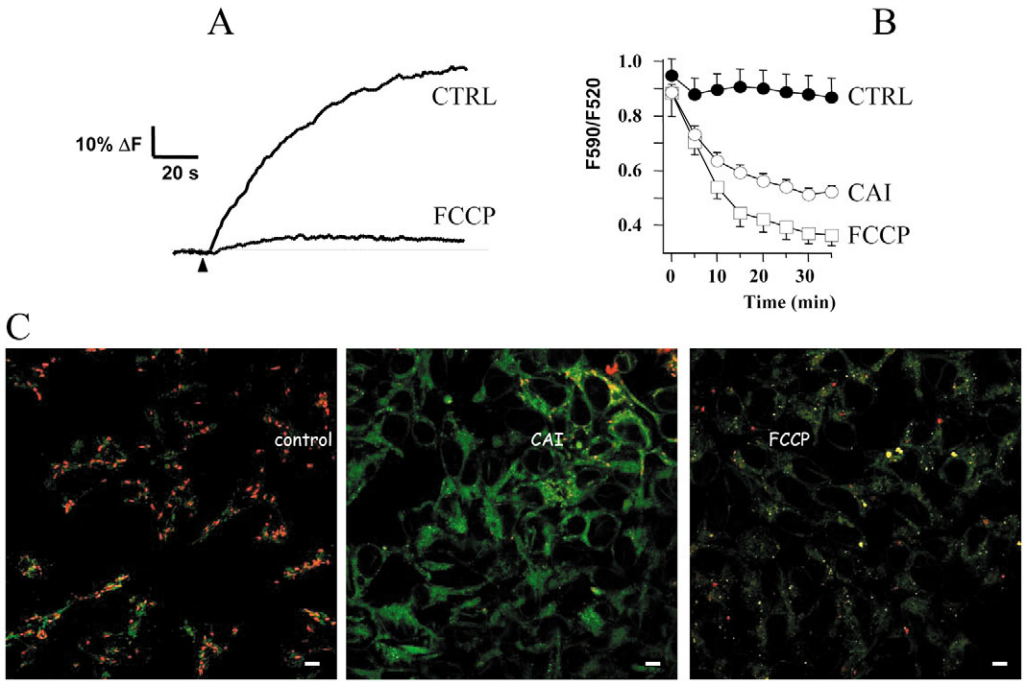

Fig. 4. Effect of CAI and FCCP on mitochondrial inner-membrane potential (ψ_m). (A) Following complete Ca^{2+} store depletion by perfusion with 10 μM TG in nominal Ca^{2+}-containing solution for about 5 minutes, 5 mM Ca^{2+} was added to the perfusate (arrowhead) evoking an increase in $[Ca^{2+}]_m$ in control cells loaded with 2 μM Rhod-2/AM. This increase was greatly attenuated in loaded cells co-treated with 10 μM TG and 20 μM FCCP. (B) Application of CAI (10 μM) or FCCP (20 μM) inhibited ψ_m compared with vehicle-treated (0.1% DMSO) controls as determined by JC-1 dye red-to-green fluorescence ratio. (C) Confocal images of JC-1-loaded (2 μg/ml) HEK-293 cells pretreated for 20 minutes with vehicle, CAI or FCCP. Bars, 10 μm.

fluorescence plate reader using the mitochondrial-selective cationic dye, JC-1. The accumulation of JC-1 in mitochondria is driven by ψ_m. At lower concentrations, JC-1 exists as a green fluorescent monomer, but at higher concentrations it aggregates as a red fluorescent form. Thus, the ratio of red-to-green fluorescence can be used to monitor ψ_m without introducing errors due to mitochondrial swelling. HEK-293 cell suspensions were treated with 10 μM CAI to assess the time course and magnitude of the acute depolarization induced by CAI. The 590/520 nm ratios were calculated at 5 minute intervals for 35 minutes following the administration of vehicle (0.1% DMSO), 20 μM FCCP or 10 μM CAI (Fig. 4B). Drugs were added just before fluorescence acquisition. CAI significantly decreased ψ_m within 5 minutes. At 15 minutes, the vehicle had not significantly altered ψ_m (0.9±0.06; n=12). Treatment with 10 μM CAI or 20 μM FCCP, a protonophore that uncouples mitochondria and abolishes ψ_m, significantly decreased the JC-1 ratio to 0.6±0.03 and 0.4±0.07, respectively, at 15 minutes (n=56 and 16; P<0.001 compared with levels in the controls). The depolarizing effect of CAI on HEK-293 cell mitochondria was validated by fluorescence imaging using confocal microscopy. JC-1-loaded control cells treated for 20 minutes with vehicle exhibited punctate red and green fluorescence, indicating a heterogeneous mitochondrial membrane potential (Fig. 4C). However, cultures that were treated for 20 minutes with 10 μM CAI or 20 μM FCCP displayed a largely diffuse green fluorescence, consistent with impairment of ψ_m (Fig. 4C).

Because JC-1 dye provides only a threshold index, rather than a graded indication, of actual mitochondrial membrane potential, we performed a set of experiments to validate our observation that CAI reduced ψ_m. Treatment with TMRE at low concentration (12.5 nM) allowed both spontaneous changes in ψ_m to be observed, as well as a reduction (or redistribution) of TMRE signal from mitochondria following treatment with 20 μM FCCP (Fig. 5A). (ROIs were placed on structures identified as mitochondria.) This method was adapted to acquire average ψ_m changes in a multi-well plate reader (that lacked high resolution imaging) by using TMRE loaded at higher concentrations (Duchen et al., 2001). In these experiments, the net cell fluorescence signal increases as dye redistributes to the cytosol and dequenches (Fig. 5B). Fig. 5C shows the averaged results of multi-well plate reader experiments where 0 or 10 μM CAI was applied to each well and the fluorescence intensity was monitored prior to and following treatment at 1 minute intervals. Similarly to JC-1 experiments, 10 μM CAI was found to significantly reduce ψ_m compared with that in the control in a time-dependent manner. For example, 10 minutes after treatment, the control value was on average 2216±140 fluorescence units whereas the value in CAI-treated cells was 4173±418 fluorescence units (n=12 and 18, respectively; P=0.001). Moreover, the effect of 10 μM CAI was not significantly different from FCCP treatment (3157±162, n=13).

CAI inhibits mitochondrial calcium import

As the robust ψ_m (~–180 mV) is the driving force for mitochondrial Ca^{2+} import, we monitored the effect of CAI on $[Ca^{2+}]_m$ using a fluorescence multi-well plate reader and permeabilized HEK-293 cells. In this experiment, cells were loaded with the mitochondrial-selective dyes Rhod-2 and MitoTracker Green prior to permeabilization. Following digitonin permeabilization in 'zero'-Ca^{2+} solution, cells were resuspended in ISS containing 30 μM Ca^{2+} with or without the addition of 10 μM CAI. To account for dye leakage or mitochondrial swelling, the Rhod-2 dye signal was measured with respect to the MitoTracker Green signal every 5 minutes for 35 minutes. CAI treatment induced ~10% loss of fluorescence over a 30 minute period compared with control mitochondria (Fig. 6A). To investigate the apparent inhibitory effect of CAI in more detail, we assessed the effect of CAI

Journal of Cell Science

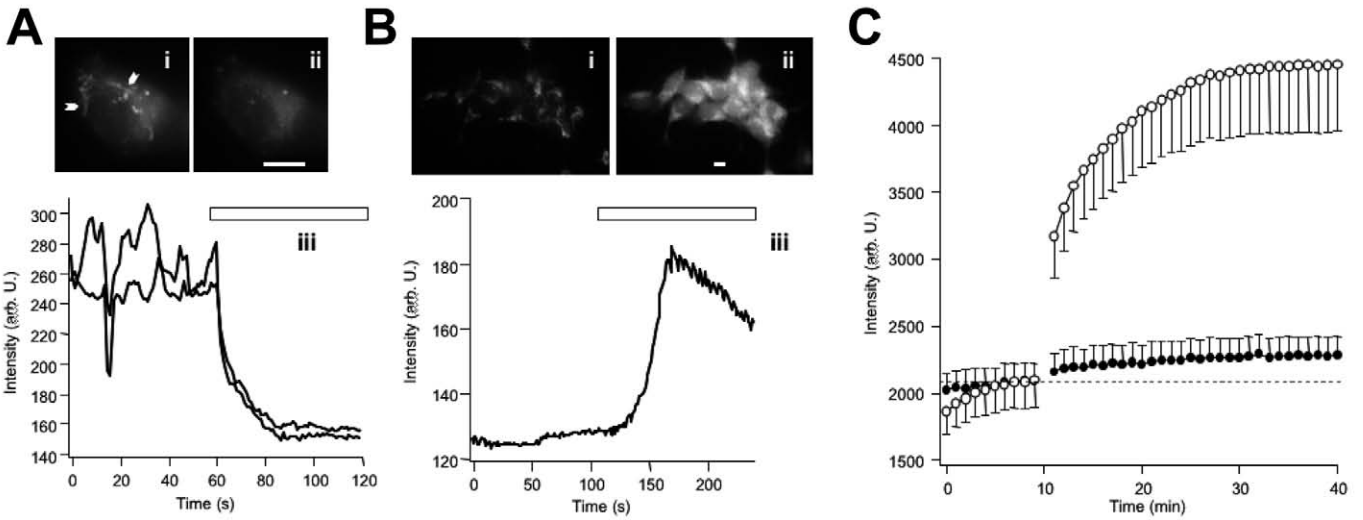

Fig. 5. CAI depolarizes the mitochondrial inner-membrane potential in a concentration-dependent manner. (A) Digital images of TMRE fluorescence in a single HEK-293 cell 60 seconds prior to (i) and 10 seconds following (ii) FCCP application (indicated by bar). (iii) Line traces of intensity changes from mitochondria indicated by white chevrons in (i). Note the spontaneous changes in ψ_m and loss of fluorescence on depolarization when TMRE was loaded at low concentration. (B) Conversely, following high concentration loading of TMRE (i), FCCP application induced an increase in fluorescence in a small cluster of HEK-293 cells (ii); a response to depolarization and unquenching of the fluorophore as dye redistributed to the cytosol. (iii) Averaged intensity trace of rises in fluorescence measured in individual cells. (C) Average fluorescence intensity changes of high concentration TMRE-loaded cells treated with vehicle only (filled symbols) or treated with 10 μM CAI (open symbols). Cell suspensions were analyzed using a multi-well fluorescence plate reader. The break in the records indicates application of the drug. Bars, 10 μm.

treatment on the rate and magnitude of changes in $[Ca^{2+}]_m$. This was done by treating cell cultures with a mixture of Rhod-2/AM, Rhod-FF/AM and Rhod-5N/AM, to load mitochondria selectively with Ca^{2+}-sensitive indicators. These cationic Rhodamine dyes preferentially localize to the mitochondria and are concentrated by mitochondrial esterases. A mixture of dyes was used so that we could follow $[Ca^{2+}]_m$ over the wide range of calcium concentrations (3-3000 μM) tested. Although we have previously observed that treatment with the muscarinic agonist carbacholamine and activation of CCE trigger an increase in $[Ca^{2+}]_m$, we chose to apply directly controlled amounts of Ca^{2+} to the cytosol and mitochondria. This approach allowed us to study the effect of CAI on $[Ca^{2+}]_m$ dynamics independently of effects on CCE. To achieve this, dye-loaded cells were permeabilized in a 'zero' (no added) Ca^{2+} ISS with 10 μM digitonin for 3 minutes at 37°C (Bruce et al., 2004). In these conditions, the plasma membrane was permeabilized, but mitochondria were left intact as determined by JC-1 fluorescence (data not shown). Moreover, permeabilization dramatically reduced the cytosolic background of the Rhodamine signal (cells that exhibited a diffuse increase in cytosolic fluorescence were not included in the estimates of $[Ca^{2+}]_m$). A representative example using permeabilized cells is shown in Fig. 6E. The punctate fluorescence represents individual or small clusters of mitochondria. Consistent with this, the fluorescent spots had an average size of 6 pixels (~1.5 μm), were colocalized with MitoTracker Green or JC-1 fluorescence and were reduced in intensity by treatment with FCCP. Regions of interest were placed randomly on individual spots and changes followed and averaged. In these cells, treatment with 300 μM Ca^{2+} produced a gradual, complex increase in $[Ca^{2+}]_m$ that reached a new steady state after several minutes. Similar experiments were performed adding various concentrations of Ca^{2+} (Fig. 6B). Set Ca^{2+} concentrations (between 3 and 3000 μM) were applied locally through a pipette placed at the measurement site and the resulting change in mitochondrial fluorescence was monitored. For each experiment, changes in fluorescence of 12 to 28 individual mitochondria/fields of view were averaged. We found that both the rate and magnitude of the change in mitochondrial fluorescence were $[Ca^{2+}]$-dependent. To quantify this relationship, the average magnitude of ΔF was determined for each condition at 300 seconds and related to the applied $[Ca^{2+}]$. Our results (Fig. 6C) indicate that in permeabilized cells, mitochondria import Ca^{2+} with an EC_{50} of ~190 μM Ca^{2+}. The average ΔF induced by 3, 30, 100, 300, 1000 and 3000 μM Ca^{2+} were 9±1%, 29±0.6%, 39±13%, 65±4%, 81±14% and 91±12%, respectively ($3 \leqslant n \leqslant 9$). However, the fact that the increase in $[Ca^{2+}]_m$ was slow compared with that induced in intact cells by agonists or CCE suggests that, although permeabilized, the added Ca^{2+} did not have unrestricted access to the cytosol. The magnitude of the $[Ca^{2+}]_m$ was lower in CAI-treated cells challenged with 30, 100 and 300 μM Ca^{2+} than in control mitochondria (Fig. 6C). The average ΔF induced by Ca^{2+} challenges of 3, 30, 100 and 300 μM were 11±2.5%, 14±4%, 23±13% and 36±9%, respectively ($5 \leqslant n \leqslant 9$), and the EC_{50} of CAI was estimated at ~180 μM.

Next, we assessed the effects of CAI treatment on the relationship between the $\Delta[Ca^{2+}]_m$ and the applied $[Ca^{2+}]$. Cells were incubated with 10 μM CAI for 15 minutes prior to permeabilization and calcium was applied in the continued presence of 10 μM CAI. Representative traces of the $\Delta[Ca^{2+}]_m$ induced by addition of 30 μM Ca^{2+} in control conditions and following CAI treatment are shown in Fig. 6D. Line traces shown in the inset of Fig. 6D represent examples of the rate and magnitude of Ca^{2+} uptake in control mitochondria and in

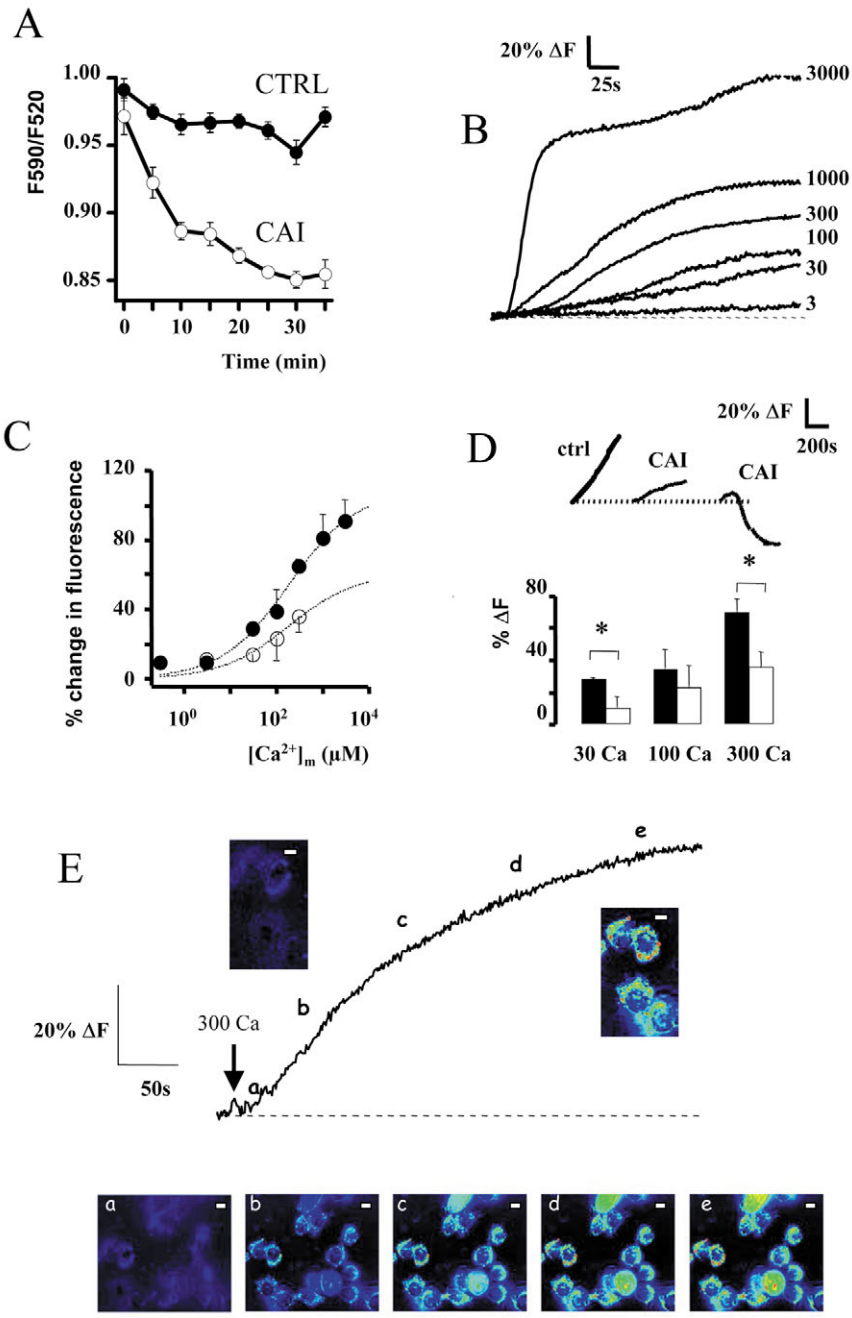

Fig. 6. Effect of CAI treatment on $[Ca^{2+}]_m$ dynamics in digitonin-permeabilized HEK-293 cells. (A) Mean Rhod-2/MitoTracker Green ratio fluorescence changes for suspensions of permeabilized HEK cells pre-treated with 30 μM Ca^{2+}. Cells were treated at time 0 with vehicle (closed circles) or 10 μM CAI (open circles) and fluorescence changes were monitored by multi-well fluorescence plate reader. (B) Changes in $[Ca^{2+}]_m$ in permeabilized HEK cells in response to intracellular saline solutions containing specific set levels of $[Ca^{2+}]$ (3-3000 μM) measured as in Fig. 3. (C) Relationship between the concentration of Ca^{2+} added and the mean change in mitochondrial fluorescence in permeabilized cells. Mitochondrial fluorescence was measured 300 seconds after adding Ca^{2+}. ○, 10 μM CAI-treated cells; ●, vehicle-treated cells. (D) Effect of pre-treatment with CAI on change in $[Ca^{2+}]_m$ induced by adding 30 μM Ca^{2+}. Representative traces are shown, demonstrating an attenuation and/or loss of mitochondrial fluorescence compared with the control. (E) Representative digital fluorescence images (a-e) of HEK cells loaded with 2 μM mixture of Rhod-2, Rhod-FF and Rhod-5N dyes (1:1:1). Cells were permeabilized with 10 μM digitonin for 3 minutes in nominal Ca^{2+} and then challenged (arrow) with the saline solution containing 300 μM free Ca^{2+}. The trace is the mean time-dependent change in fluorescence measured from individual puncta (see insets). Ca^{2+}-containing solutions were applied locally (about 50-100 μm from the field of view) using a pressure-driven perfusion system. Bars, 10 μm.

two other experiments where mitochondrial uptake was diminished or even decreased below resting fluorescence levels following CAI treatment. The rate and magnitude of $\Delta[Ca^{2+}]_m$ following CAI treatment were generally lower than those measured in control conditions. In some experiments, fluorescence was rapidly lost, suggesting that the permeability transition pore (PTP) had been activated. The PTP has been shown to be activated by elevated $[Ca^{2+}]_m$ and by the generation of reactive oxygen species (ROS).

Effects of CAI and 2-APB on HEK-293 cell proliferation

Cell proliferation is tightly dependent on calcium influx (Munaron et al., 2004) and we recently showed that CAI blocks both proliferation and CCE in human hepatoma cells (Enfissi et al., 2004). We assessed the proliferation of HEK-293 cells by measuring the incorporation of [^{3}H]thymidine. Cells were first incubated for 24 hours in the presence of 10% FCS. The external medium was then replaced by fresh medium supplemented with various concentrations of CAI or 2-APB and the cells were incubated for a further 24 hours. CAI and 2-APB blocked the incorporation of [^{3}H]thymidine into HEK-293 cells, with an IC_{50} of 1.6 and 50 μM, respectively (Fig. 7A,B), whereas the vehicle (0.1% DMSO) had no effect (data not shown).

Discussion

Several studies have shown that cell proliferation is associated with an increase in CCE (Golovina, 1999; Golovina et al.,

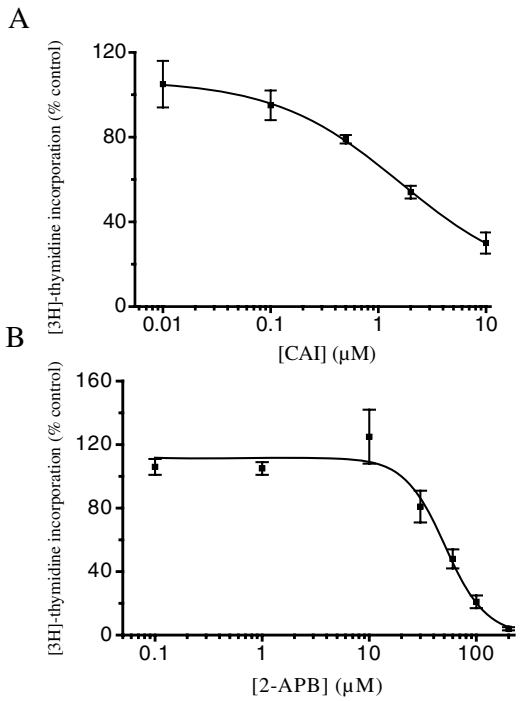

Fig. 7. Inhibition of [^{3}H]thymidine incorporation by CAI and 2-APB in HEK-293 cells. HEK-293 cells were incubated for 24 hours in the presence of 10% FCS and for a further 24 hours in the presence of various concentrations of CAI (A) and 2-APB (B). Results are expressed as a percentage of [^{3}H]thymidine incorporation in the absence of CAI and 2-APB in both conditions. The result for each experiment is the mean of four samples and each point on the plot is the mean±s.e.m. of three or four independent experiments.

2001; Sweeney et al., 2002; Yu et al., 2003). In this work, we demonstrated that blocking CCE with CAI and 2-APB inhibits the proliferation of HEK-293 cells with similar potency to human hepatoma cell lines (Enfissi et al., 2004).

Functional mitochondria with the ability to take up calcium to buffer large increases in cytosolic calcium concentration (Jacobson and Duchen, 2004) are important in the overall control of CCE. Thus, as CCE is inactivated by high intracellular calcium concentrations, it is likely that those mitochondria that are located near to calcium channels (Varadi et al., 2004), reduce this inactivation. Calcium hotspots as high as 200-300 μM measured in front of calcium channels (Llinas et al., 1992) are in the range of concentrations detected by mitochondria. Furthermore, the slow rate of addition of calcium in our experiments probably leads to an overestimation of the measured value for mitochondrial calcium import. Consistent with this, inhibition of mitochondrial Ca^{2+} uptake by compounds that dissipate the mitochondrial membrane potential (such as oligomycin or CCCP) unmasks the Ca^{2+}-dependent inactivation of CCE, resulting in a clear inhibition of calcium entry (Gilabert and Parekh, 2000; Glitsch et al., 2002; Hoth et al., 2000; Hoth et al., 1997). Mitochondrial respiration was first inhibited approximately 30 seconds after the addition of CAI at concentrations used to block CCE in Hep G2 cells (T.C., unpublished data). The time-dependent nature of the effects of CAI on mitochondria function in HEK-293 cells strongly suggest that CCE inhibition results from an alteration in the ability of mitochondria to buffer cell calcium. Thus, the CAI-induced block of CCE may be due to the direct blockage of calcium channels or to an indirect effect involving mitochondria and inactivation of the current by internal calcium. CAI does not block I_{SOC} when applied at the peak of the current, ruling out a direct block of the channels. Furthermore, increasing the calcium buffering capacity of the cell has been shown to prevent CCE inactivation by mitochondria inhibitors (Glitsch et al., 2002). We observed that 5 μM CAI reduced the SOC amplitude by about 50% whereas it totally blocked CCE in cell suspensions in which internal calcium is not buffered by EGTA. However, CCE was not sustained and declined to an intermediate plateau phase in HEK-293 cell suspensions. Hence, addition of CAI at the plateau has little effect on the amplitude of the calcium response. However, in human Huh-7 hepatoma cells, in which the plateau phase is often maintained at its maximal level, CAI reduces the amplitude of the CCE (Enfissi et al., 2004). Alternatively, CAI may alter one of the mechanisms of SOC activation (Venkatachalam et al., 2002), thus making the drug less effective when applied at the peak of the current activated by store depletion in whole-cell voltage-clamp experiments.

Our data clearly show that CAI does not inhibit Ca^{2+} entry via the ARC channels. It has also been shown that 2-APB has different effects on CCE and ARC channels (Mignen and Thompson et al., 2003). In Huh-7 cells, addition of 10% FCS evokes sustained increases in $[Ca^{2+}]_i$, which were sensitive to external calcium, 2-APB and CAI (Enfissi et al., 2004). This suggests that CCE is the only calcium entry pathway activated at this serum concentration. Although CAI blocks cell proliferation induced by 10% FCS, we have no evidence that the effects of lower concentrations of serum would be sensitive to CAI. Hence, although our results clearly show that CCE is implied in cell proliferation, we cannot exclude the possibility that ARC or DAG-activated NCCE channels play a role in cell proliferation at lower serum concentrations.

Precisely how calcium influx via CCE influences cell proliferation is unclear. However, the progression through the cell cycle is regulated by several cyclins. CCE, as opposed to NCCE, activates calcineurin (Mignen et al., 2003), which in turn allows expression of cyclin A and E (Tomono et al., 1998), and cyclin D2 induction is abolished in the presence of CCE blockers (Glassford et al., 2003). Therefore, it is likely that calcium influx may block cell proliferation by preventing cyclin induction.

In summary, the reduced cell proliferation rate associated with CCE inhibition reflects the well-described antiproliferative and antimetastasic properties that have led to CAI being proposed as a potential drug for cancer treatment (Kohn and Liotta, 1995; Patton et al., 2003). Moreover, the fact that CAI clearly inhibits CCE emphasizes the relationships between this specific calcium entry pathway and cell proliferation. However, our unexpected finding that the mitochondria represent a major target for CAI will probably limit its use in the treatment of cancers. Moreover, our results reinforce the crucial role that mitochondria play in the induction of cancer as membrane potential breakdown, in addition to the triggering of apoptosis (Henry-Mowatt et al., 2004; Tirosh et al., 2003), induces an inhibition of cell proliferation. The design of more specific CCE blockers holds much promise for the development of potential anticancer

therapies, but this will almost certainly not be possible before the molecular identification of the specific calcium channels involved in this pathway.

This work was supported by the American Heart Association (D.R.G., grant 0130231N), National Institutes of Health (D.R.G., grant DE14756 and GM040457 to T.J.S.), Association pour la Recherche contre le Cancer (T.C., ARC 5621 and 4615) and Comité de l'Essonne de la Ligue contre le Cancer (T.C.). CAI was kindly provided by the Developmental Therapeutics Program, National Cancer Institute. We also thank Josiane Simon (INSERM U442, Orsay France), Juan Zhang and Arun Ragothaman (Department of Neuroscience, Medical College of Ohio, Toledo, Ohio, USA) for valuable assistance with some of the experiments.

References

Alessandro, R., Masiero, L., Liotta, L. A. and Kohn, E. C. (1996). The role of calcium in the regulation of invasion and angiogenesis. *In Vivo* **10**, 153-160.

Bird, G. S., Aziz, O., Lievremont, J. P., Wedel, B. J., Trebak, M., Vazquez, G. and Putney, J. W., Jr (2004). Mechanisms of phospholipase C-regulated calcium entry. *Curr. Mol. Med.* **4**, 291-301.

Bruce, J. I., Giovannucci, D. R., Blinder, G., Shuttleworth, T. J. and Yule, D. I. (2004). Modulation of [Ca2+]i signaling dynamics and metabolism by perinuclear mitochondria in mouse parotid acinar cells. *J. Biol. Chem.* **279**, 12909-12917.

Duchen, M. R., Jacobson, J., Keelan, J., Mojet, M. H. and Vergun, O. (2001). Functional imaging of mitochondrial within cells. In *Methods in Cellular Imaging* (ed. A. Periasamy), pp. 88-111. New York: Oxford University Press.

Enfissi, A., Prigent, S., Colosetti, P. and Capiod, T. (2004). The blocking of capacitative calcium entry by 2-aminoethyl diphenylborate (2-APB) and carboxyamidotriazole (CAI) inhibits proliferation in Hep G2 and Huh-7 human hepatoma cells. *Cell Calcium* **36**, 459-467.

Felder, C. C., Ma, A. L., Liotta, L. A. and Kohn, E. C. (1991). The antiproliferative and antimetastatic compound L651582 inhibits muscarinic acetylcholine receptor-stimulated calcium influx and arachidonic acid release. *J. Pharmacol. Exp. Ther.* **257**, 967-971.

Gilabert, J. A. and Parekh, A. B. (2000). Respiring mitochondria determine the pattern of activation and inactivation of the store-operated Ca(2+) current I(CRAC). *EMBO J.* **19**, 6401-6407.

Glassford, J., Soeiro, I., Skarell, S. M., Banerji, L., Holman, M., Klaus, G. G., Kadowaki, T., Koyasu, S. and Lam, E. W. (2003). BCR targets cyclin D2 via Btk and the p85alpha subunit of PI3-K to induce cell cycle progression in primary mouse B cells. *Oncogene* **22**, 2248-2259.

Glitsch, M. D., Bakowski, D. and Parekh, A. B. (2002). Store-operated Ca2+ entry depends on mitochondrial Ca2+ uptake. *EMBO J.* **21**, 6744-6754.

Golovina, V. A. (1999). Cell proliferation is associated with enhanced capacitative Ca(2+) entry in human arterial myocytes. *Am. J. Physiol.* **277**, C343-C349.

Golovina, V. A., Platoshyn, O., Bailey, C. L., Wang, J., Limsuwan, A., Sweeney, M., Rubin, L. J. and Yuan, J. X. (2001). Upregulated TRP and enhanced capacitative Ca(2+) entry in human pulmonary artery myocytes during proliferation. *Am. J. Physiol. Heart Circ. Physiol.* **280**, H746-H755.

Haverstick, D. M., Heady, T. N., Macdonald, T. L. and Gray, L. S. (2000). Inhibition of human prostate cancer proliferation in vitro and in a mouse model by a compound synthesized to block Ca2+ entry. *Cancer Res.* **60**, 1002-1008.

Henry-Mowatt, J., Dive, C., Martinou, J. C. and James, D. (2004). Role of mitochondrial membrane permeabilization in apoptosis and cancer. *Oncogene* **23**, 2850-2860.

Hoth, M., Fanger, C. M. and Lewis, R. S. (1997). Mitochondrial regulation of store-operated calcium signaling in T lymphocytes. *J. Cell Biol.* **137**, 633-648.

Hoth, M., Button, D. C. and Lewis, R. S. (2000). Mitochondrial control of calcium-channel gating: a mechanism for sustained signaling and transcriptional activation in T lymphocytes. *Proc. Natl. Acad. Sci. USA* **97**, 10607-10612.

Hussain, M. M., Kotz, H., Minasian, L., Premkumar, A., Sarosy, G., Reed, E., Zhai, S., Steinberg, S. M., Raggio, M., Oliver, V. K. et al. (2003). Phase II trial of carboxyamidotriazole in patients with relapsed epithelial ovarian cancer. *J. Clin. Oncol.* **21**, 4356-4363.

Jacobson, J. and Duchen, M. R. (2004). Interplay between mitochondria and cellular calcium signalling. *Mol. Cell. Biochem.* **256-257**, 209-218.

Kohn, E. C. and Liotta, L. A. (1990). L651582: a novel antiproliferative and antimetastasis agent. *J. Natl. Cancer Inst.* **82**, 54-60.

Kohn, E. C. and Liotta, L. A. (1995). Molecular insights into cancer invasion: strategies for prevention and intervention. *Cancer Res.* **55**, 1856-1862.

Kohn, E. C., Figg, W. D., Sarosy, G. A., Bauer, K. S., Davis, P. A., Soltis, M. J., Thompkins, A., Liotta, L. A. and Reed, E. (1997). Phase I trial of micronized formulation carboxyamidotriazole in patients with refractory solid tumors: pharmacokinetics, clinical outcome, and comparison of formulations. *J. Clin. Oncol.* **15**, 1985-1993.

Llinas, R., Sugimori, M. and Silver, R. B. (1992). Microdomains of high calcium concentration in a presynaptic terminal. *Science* **256**, 677-679.

Mignen, O. and Shuttleworth, T. J. (2000). I(ARC), a novel arachidonate-regulated, noncapacitative Ca(2+) entry channel. *J. Biol. Chem.* **275**, 9114-9119.

Mignen, O., Thompson, J. L. and Shuttleworth, T. J. (2001). Reciprocal regulation of capacitative and arachidonate-regulated noncapacitative Ca2+ entry pathways. *J. Biol. Chem.* **276**, 35676-35683.

Mignen, O., Thompson, J. L. and Shuttleworth, T. J. (2003). Calcineurin directs the reciprocal regulation of calcium entry pathways in nonexcitable cells. *J. Biol. Chem.* **278**, 40088-40096.

Mignen, O., Thompson, J. L., Yule, D. I. and Shuttleworth, T. J. (2005a). Agonist activation of arachidonate-regulated Ca2+-selective (ARC) channels in murine parotid and pancreatic acinar cells. *J. Physiol.* **564**, 791-801.

Mignen, O., Thompson, J. L., Yule, D. I. and Shuttleworth, T. J. (2005b). Agonist activation of ARC channels in parotid and pancreatic acinar cells. *J. Physiol*. **564**, 791-801

Munaron, L., Antoniotti, S., Fiorio Pla, A. and Lovisolo, D. (2004). Blocking Ca2+entry: a way to control cell proliferation. *Curr. Med. Chem.* **11**, 1533-1543.

Parekh, A. B. and Putney, J. W., Jr (2005). Store-operated calcium channels. *Physiol. Rev.* **85**, 757-810.

Patton, A. M., Kassis, J., Doong, H. and Kohn, E. C. (2003). Calcium as a molecular target in angiogenesis. *Curr. Pharm. Des.* **9**, 543-551.

Peppiatt, C. M., Collins, T. J., Mackenzie, L., Conway, S. J., Holmes, A. B., Bootman, M. D., Berridge, M. J., Seo, J. T. and Roderick, H. L. (2003). 2-Aminoethoxydiphenyl borate (2-APB) antagonises inositol 1,4,5-trisphosphate-induced calcium release, inhibits calcium pumps and has a use-dependent and slowly reversible action on store-operated calcium entry channels. *Cell Calcium* **34**, 97-108.

Shuttleworth, T. J. and Thompson, J. L. (1999). Discriminating between capacitative and arachidonate-activated Ca(2+) entry pathways in HEK293 cells. *J. Biol. Chem.* **274**, 31174-31178.

Sweeney, M., Yu, Y., Platoshyn, O., Zhang, S., McDaniel, S. S. and Yuan, J. X. (2002). Inhibition of endogenous TRP1 decreases capacitative Ca2+ entry and attenuates pulmonary artery smooth muscle cell proliferation. *Am. J. Physiol. Lung Cell Mol. Physiol.* **283**, L144-L155.

Thebault, S., Roudbaraki, M., Sydorenko, V., Shuba, Y., Lemonnier, L., Slomianny, C., Dewailly, E., Bonnal, J. L., Mauroy, B., Skryma, R. et al. (2003). Alpha1-adrenergic receptors activate Ca(2+)-permeable cationic channels in prostate cancer epithelial cells. *J. Clin. Invest.* **111**, 1691-1701.

Tirosh, O., Aronis, A. and Melendez, J. A. (2003). Mitochondrial state 3 to 4 respiration transition during Fas-mediated apoptosis controls cellular redox balance and rate of cell death. *Biochem. Pharmacol.* **66**, 1331-1334.

Tomono, M., Toyoshima, K., Ito, M., Amano, H. and Kiss, Z. (1998). Inhibitors of calcineurin block expression of cyclins A and E induced by fibroblast growth factor in Swiss 3T3 fibroblasts. *Arch. Biochem. Biophys.* **353**, 374-378.

Varadi, A., Cirulli, V. and Rutter, G. A. (2004). Mitochondrial localization as a determinant of capacitative Ca(2+) entry in HeLa cells. *Cell Calcium* **36**, 499-508.

Venkatachalam, K., van Rossum, D. B., Patterson, R. L., Ma, H. T. and Gill, D. L. (2002). The cellular and molecular basis of store-operated calcium entry. *Nat. Cell Biol.* **4**, E263-E272.

Yu, Y., Sweeney, M., Zhang, S., Platoshyn, O., Landsberg, J., Rothman, A. and Yuan, J. X. (2003). PDGF stimulates pulmonary vascular smooth muscle cell proliferation by upregulating TRPC6 expression. *Am. J. Physiol. Cell Physiol.* **284**, C316-C330.